

Spin Crossover in a Four-Coordinate Iron(II) Complex

Jeremiah J. Scepaniak,[†] T. David Harris,[‡] Carola S. Vogel,[§] Jörg Sutter,[§] Karsten Meyer,^{*,§} and Jeremy M. Smith^{*,†}

[†]Department of Chemistry and Biochemistry, New Mexico State University, Las Cruces, New Mexico 88003, United States

[‡]Department of Chemistry, University of California, Berkeley, California 94720, United States

[§]Department of Chemistry and Pharmacy, Friedrich-Alexander-University Erlangen-Nuremberg, Egerlandstr. 1, 91058 Erlangen, Germany

S Supporting Information

ABSTRACT: The four-coordinate iron(II) phosphoraniminato complex $\text{PhB}(\text{MesIm})_3\text{Fe}-\text{N}=\text{PPh}_3$ undergoes an $S = 0$ to $S = 2$ spin transition with $T_C = 81$ K, as determined by variable-temperature magnetic measurements and Mössbauer spectroscopy. Variable-temperature single-crystal X-ray diffraction revealed that the $S = 0$ to $S = 2$ transition is associated with an increase in the Fe–C and Fe–N bond distances and a decrease in the N–P bond distance. These structural changes have been interpreted in terms of electronic structure theory.

Spin-crossover complexes are characterized by the ability of a transition-metal center to undergo a change in electronic configuration in response to an external input such as heat, light, pressure, or changes in magnetic field.¹ Since the molecular bistability of spin-crossover molecules is associated with a lack of fatigue, there is considerable interest for applications such as sensors and digital memory.²

Spin crossover is typically observed in first-row transition-metal complexes having d^4 – d^7 electron counts. The largest group of spin-crossover complexes consists of mononuclear iron(II) complexes with an FeN_6 coordination environment.³ In these complexes, the $S = 0$ (t_{2g}^6) to $S = 2$ ($t_{2g}^4e_g^2$) transition is generally accompanied by an increase of ~ 0.1 Å in the Fe–N bond lengths. While a small number of higher-coordinate spin-crossover complexes are known, lower-coordinate iron(II) complexes almost invariably assume a high-spin electronic configuration.⁴ Indeed, reports of spin crossover in complexes with coordination numbers lower than 4 are very rare.^{4–6}

We report herein the first example of a four-coordinate iron(II) complex that undergoes spin crossover.⁷ The transition from $S = 0$ to $S = 2$ has been characterized by dc magnetic susceptibility measurements and Mössbauer spectroscopy. In addition, variable-temperature single-crystal X-ray diffraction has provided insights into the structural changes associated with the spin transition. Moreover, the electronic structures of the two spin states have been determined by density functional theory (DFT). Finally, both the tris(carbene)borate and phosphoraniminato ligands lend themselves to facile synthetic modification, thus highlighting the potential of this system for tunable spin-crossover behavior.

Reaction of the iron(IV) nitrido complex $\text{PhB}(\text{MesIm})_3\text{-Fe}\equiv\text{N}^8$ with PPh_3 resulted in the formation of yellow-green

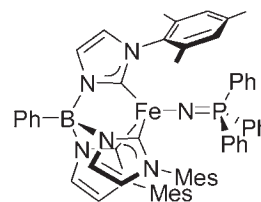


Figure 1. $\text{PhB}(\text{MesIm})_3\text{Fe}-\text{N}=\text{PPh}_3$ (**1**).

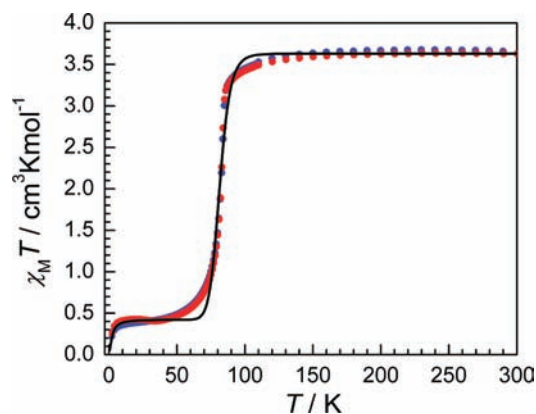


Figure 2. Variable-temperature dc susceptibility data collected for **1** while warming (red) and cooling (blue) under an applied field of 1 T. The solid black line corresponds to fits to the data, as described in the text.

$\text{PhB}(\text{MesIm})_3\text{Fe}-\text{N}=\text{PPh}_3$ (**1**) in high yield (Figure 1), similar to our previous report on the synthesis of $\text{PhB}(\text{tBuIm})_3\text{Fe}-\text{N}=\text{PPh}_3$.⁹ The complex was structurally characterized at multiple temperatures (see below). In solution at ambient temperature, **1** has a high-spin electronic configuration ($S = 2$) characterized by a paramagnetically shifted ^1H NMR spectrum and a solution magnetic moment [$5.2(3)\mu_B$].

The solid-state magnetic behavior of **1** was probed by variable-temperature dc susceptibility measurements on a polycrystalline sample under an applied field of 1 T. As shown in Figure 2, $\chi_M T = 3.63$ $\text{cm}^3 \cdot \text{mol}^{-1} \cdot \text{K}$ at 300 K, consistent with an $S = 2$ state with $g = 2.2$. There was little change in $\chi_M T$ as the temperature was decreased to 150 K, at which point $\chi_M T$

Received: January 13, 2011

Published: March 02, 2011

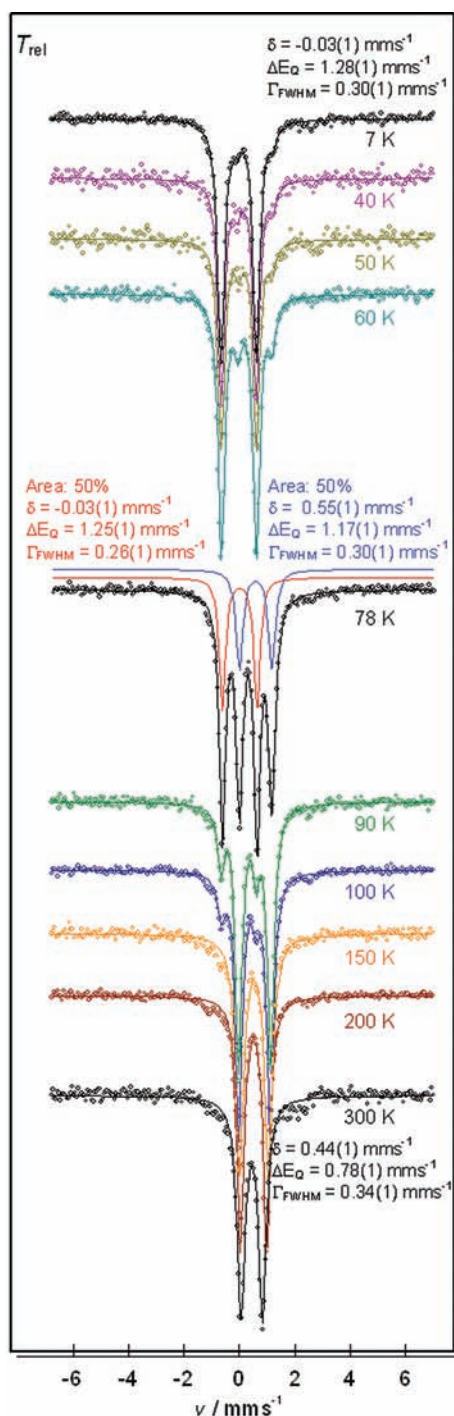


Figure 3. Variable-temperature, zero-field Mössbauer spectra of **1**.

started to gradually decrease before dropping precipitously at 81 K. From 50 to 10 K, $\chi_M T$ decreased slightly (from 10 to 50 K, the average value of $\chi_M T$ was $0.42 \text{ cm}^3 \cdot \text{mol/K}$), and this was followed by a rapid decrease below 10 K, likely due to Zeeman and zero-field splitting. The $\chi_M T$ curve was essentially identical when the temperature was increased from 2 to 300 K, and notably, no hysteresis was evident at the applied sweep rates.

The precipitous drop in $\chi_M T$ at 81 K is indicative of a transition from a thermally excited high-spin $S = 2$ state at high temperature to a low-spin $S = 0$ ground state at low temperature.

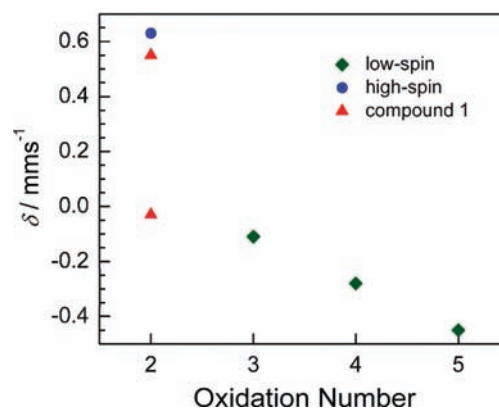


Figure 4. Isomer shifts as a function of oxidation state for iron tris(carbene)borate complexes $\text{PhB(RIm)}_3\text{FeX}$ ($\text{R} = \text{tBu, Mes}$). For details, see the Supporting Information.¹⁹

The average $\chi_M T$ value of $0.42 \text{ cm}^3 \cdot \text{mol/K}$ below 50 K corresponds to 12% of the sample retaining a high-spin configuration at low temperature. Modeling the $\chi_M T$ data according to a Boltzmann distribution of spin states provided the values $\Delta H = 1190 \text{ cm}^{-1}$ and $T_C = 81 \text{ K}$.^{10–12} In addition, independently modeling the data below 20 K using MAGPACK¹³ provided an axial zero-field splitting parameter of $|D| = 5(2) \text{ cm}^{-1}$.¹²

The spin-state changes were confirmed by variable-temperature zero-field Mössbauer spectroscopy (Figure 3). At 7 K, a solid sample of **1** showed one major quadrupole doublet with an isomer shift of $\delta = -0.03(1) \text{ mm/s}$ and a quadrupole splitting of $\Delta E_Q = 1.28(1) \text{ mm/s}$ (93%). In addition, a minor feature that integrated to $\sim 7\%$ was observed as a shoulder on the high-energy flank of the main doublet. This latter signal grew in as the temperature was increased from 7 to 40, 50, and 60 K. At 78 K, two sharp, equally intense quadrupole doublets with $\delta = -0.03(1) \text{ mm/s}$, $\Delta E_Q = 1.25(1) \text{ mm/s}$ and $\delta = 0.55(1) \text{ mm/s}$, $\Delta E_Q = 1.17(1) \text{ mm/s}$ were observed. This latter doublet continued to grow in as the temperature was gradually increased to 90, 100, and 150 K, where the spectrum showed one doublet only [$\delta = 0.53(1) \text{ mm/s}$, $\Delta E_Q = 1.05(1) \text{ mm/s}$], characteristic of a high-spin Fe(II) [$\text{PhB(MesIm)}_3\text{FeX}$] species (Figure 4). In agreement with the dc susceptibility data, this doublet has been assigned to the high-spin state of **1**, with Mössbauer parameters of $\delta = 0.44(1) \text{ mm/s}$ and $\Delta E_Q = 0.78(1) \text{ mm/s}$ at 300 K.

The structural variation associated with the spin-state change was established by X-ray crystallography (Figure 5). The solid-state structure of **1** at 150 K, where the high-spin state is fully populated, shows metrical parameters similar to those of other tris(carbene)borate iron(II) complexes. For example, the Fe–C bond lengths [average $2.085(2) \text{ \AA}$] are similar to those in the related iron(II) complex $\text{PhB(MesIm)}_3\text{FeCl}$.⁸ It is notable that the Fe–N bond in **1** is slightly shorter than that in the closely related high-spin complex $\text{PhB}(\text{tBuIm})_3\text{Fe-N=PPh}_3$,⁹ while the N–P bond is slightly longer. This difference is presumably a consequence of the different steric properties of the two tris(carbene)borate ligands.

The solid-state structure of **1** was also determined at 30 K, where mostly the low-spin $S = 0$ ground state is populated. At this temperature, the Fe–C bond lengths are over 0.1 \AA shorter than in the high-temperature structure. In addition, there is a smaller but significant reduction in the Fe–N bond length (0.05 \AA) along with a less pronounced lengthening of the N–P bond

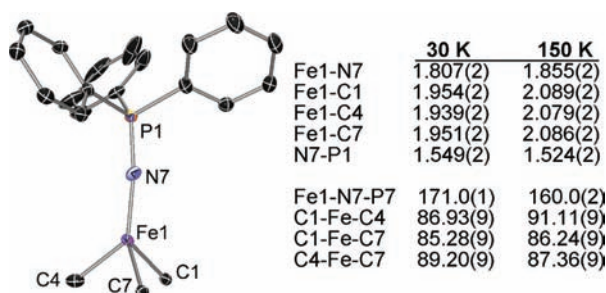


Figure 5. (left) Structural representation of the core structure of **1** at 30 K. Thermal ellipsoids are shown at 50% probability, and hydrogen atoms and most of the tris(carbene)borate ligand have been omitted for clarity. (right) Comparison of selected bond lengths (Å) and bond angles (deg) for **1** at 30 and 150 K (see the Supporting Information for details).

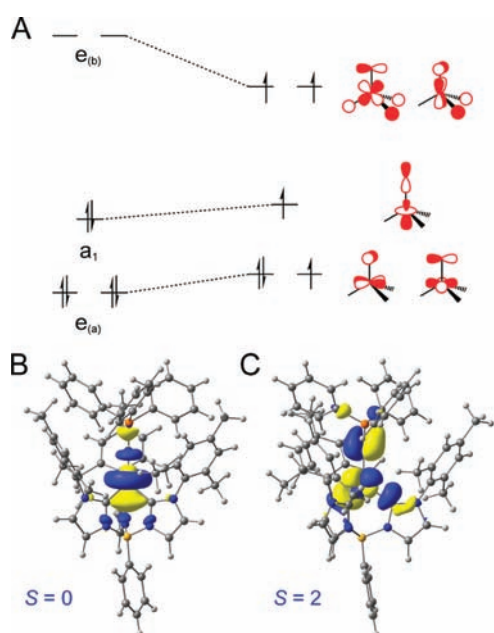


Figure 6. (A) Qualitative orbital correlation diagram for the $S = 0$ to $S = 2$ transition in **1**. (B, C) Highest occupied molecular orbitals for the (B) $S = 0$ and (C) $S = 2$ spin states as calculated using DFT methods. See the text for details.

(0.03 Å). While the Fe–N–P bond angle is greater at 30 K, the possibility that solid-state packing forces are responsible for this change cannot be discounted.¹⁴

The observed structural changes can be understood in terms of an orbital correlation diagram (Figure 6A). In idealized C_{3v} symmetry, the metal d orbitals of **1** transform as $1a_1 + 2e$, similar to the case of other pseudotetrahedral complexes. The a_1 and $e_{(a)}$ sets of orbitals are nonbonding, while the $e_{(b)}$ orbitals have σ^* interactions with the supporting tris(carbene)borate ligand and π^* interactions with the axial phosphoraniminato ligand. The strongly donating tris(carbene)borate ligand destabilizes the $e_{(b)}$ orbitals, resulting in a relatively large energy gap between them and the a_1 orbital.^{15,16} The $S = 0$ to $S = 2$ spin transition therefore transfers two electrons from nonbonding to antibonding orbitals, resulting in longer Fe–C and Fe–N bonds. The dissimilar antibonding interactions result in greater elongation of the Fe–C bonds (σ^*) than of the Fe–N bond (π^*). We note that the low-

spin state is related to the four-coordinate tris(phosphino)borate iron(II) imido complex $[\text{PhB}(\text{CH}_2\text{PPh}_2)_3\text{Fe}\equiv\text{NAd}]^-$, which also has an $S = 0$ ground state.¹⁷

The results of electronic structure calculations are consistent with the qualitative orbital picture. Geometry optimization of the two spin states using DFT methods [BPW91/6-31G(d)//6-311G(d,f)] provided structures in reasonable agreement with the crystallographic data.^{12,18} Importantly, the calculations reproduced the observed structural changes, with the longer Fe–N and Fe–C bonds in the high-spin state and a longer N–P bond in the low-spin state. Furthermore, the nature of the frontier orbitals agreed with the qualitative MO description. Thus, for $S = 0$, the HOMO has a_1 symmetry (Figure 6 B), while for $S = 2$, the HOMO has e symmetry (Figure 6 C). An additional insight from these calculations is that the shorter P–N bond length in the high-spin state is due to the P–N π -bonding contribution to the $e_{(b)}$ orbitals.

In summary, we have characterized the first example of spin crossover in a four-coordinate iron(II) complex. A combination of SQUID magnetometry, Mössbauer spectroscopy, X-ray crystallography, and electronic structure theory has provided unambiguous evidence for a metal-based spin transition with $T_C = 81$ K. It is likely that the robust tris(carbene)borate ligand platform will stabilize other iron(II) spin-crossover complexes that can be accessed by substitutions of the axial ligand. Moreover, the electronic structure predicts that the spin-crossover temperature can be modulated by changes to the π -acceptor properties of the axial ligand. Studies to investigate these hypotheses are underway.

■ ASSOCIATED CONTENT

S Supporting Information. Full experimental and computational details, complete ref 7, crystallographic data (CIF). This material is available free of charge via the Internet at <http://pubs.acs.org>.

■ AUTHOR INFORMATION

Corresponding Author

karsten.meyer@chemie.uni-erlangen.de; jesmith@nmsu.edu

■ ACKNOWLEDGMENT

J.M.S. thanks DOE-BES (DE-FG02-08ER15996) and the Camille and Henry Dreyfus Foundation for funding. K.M. thanks the University of Erlangen-Nuremberg and the DFG for generous start-up funds. T.D.H. thanks Tyco Electronics for a predoctoral fellowship.

■ REFERENCES

- Gütlich, P.; Goodwin, H. A. *Top. Curr. Chem.* **2004**, *233*, 1–47.
- Létard, J.-F.; Guionneau, P.; Goux-Capes, L. *Top. Curr. Chem.* **2004**, *235*, 221–249.
- Halcrow, M. A. *Polyhedron* **2007**, *26*, 3523–3576.
- Spin crossover in five-coordinate iron(II) complexes: (a) Bacci, M.; Midollini, S.; Stoppioni, P.; Sacconi, L. *Inorg. Chem.* **1973**, *12*, 1801–1805. (b) Li, J.; Lord, R. L.; Noll, B. C.; Baik, M.-H.; Schulz, C. B.; Scheidt, W. R. *Angew. Chem., Int. Ed.* **2008**, *47*, 10144–10146.
- Spin crossover in five-coordinate iron(III) porphyrin complexes: Nakamura, M. *Coord. Chem. Rev.* **2006**, *250*, 2271–2294.
- (a) Jenkins, D. M.; Peters, J. C. *J. Am. Chem. Soc.* **2003**, *125*, 11162–11163. (b) Jenkins, D. M.; Peters, J. C. *J. Am. Chem. Soc.*

2005, 127, 7148–7165. (c) Ni, C.; Fettinger, J. C.; Long, G. J.; Power, P. P. *Inorg. Chem.* **2009**, 48, 2443–2448.

(7) A pressure-induced $S = 2$ to $S = 1$ spin transition in a square-planar iron(II) oxide material: Kawakami, T.; et al. *Nat. Chem.* **2009**, 1, 371–376.

(8) Scepaniak, J. J.; Young, J. A.; Bontchev, R. P.; Smith, J. M. *Angew. Chem., Int. Ed.* **2009**, 48, 3158–3160.

(9) Scepaniak, J. J.; Fulton, M. D.; Bontchev, R. P.; Duesler, E. N.; Kirk, M. L.; Smith, J. M. *J. Am. Chem. Soc.* **2008**, 130, 10515–10517.

(10) Kahn, O. *Molecular Magnetism*; VCH: New York, 1993.

(11) These T_C and ΔH values give $\Delta S = 21 \text{ cm}^{-1}$.

(12) Full details are provided in the Supporting Information.

(13) Borrás-Almenar, J. J.; Clemente-Juan, J. M.; Coronado, E.; Tsukerblat, B. S. *J. Comput. Chem.* **2001**, 22, 985–991.

(14) Two different Fe–N–P bond angles [167.8(1) and 177.6(1)°] were observed in the solid-state structure of the high-spin complex $\text{PhB}(\text{tBuIm})_3\text{Fe–N}=\text{PPh}_3$, suggesting a low barrier to bending about this linkage (see ref 9).

(15) For a more detailed discussion of the nature of the a_1 orbital, see ref 9 and: Tangen, E.; Conradie, J.; Ghosh, A. *J. Chem. Theory Comput.* **2007**, 3, 448–457.

(16) Alvarez, S.; Cireca, J. *Angew. Chem., Int. Ed.* **2006**, 45, 3012–3020.

(17) Brown, S. D.; Peters, J. C. *J. Am. Chem. Soc.* **2005**, 127, 1913–1923.

(18) The electronic structures were also calculated using the B3LYP functional, but the BPW91 functional predicted the correct ground state.

(19) Scepaniak, J. J.; Vogel, C. S.; Khusniyarov, M. M.; Heinemann, F. W.; Meyer, K.; Smith, J. M. *Science* **2011**, 331, 1049–1052.